Science Advances
AAAS

Supplementary Materials for

A human mucosal melanoma organoid platform for modeling tumor heterogeneity and exploring immunotherapy combination options

Lulu Sun *et al.*

Corresponding author: Shuyang Sun, sunshuyang@sjtu.edu.cn

Sci. Adv. **9**, eadg6686 (2023)
DOI: 10.1126/sciadv.adg6686

The PDF file includes:

Figs. S1 to S7
Legends for tables S1 to S7

Other Supplementary Material for this manuscript includes the following:

Tables S1 to S7

Supplementary Figures

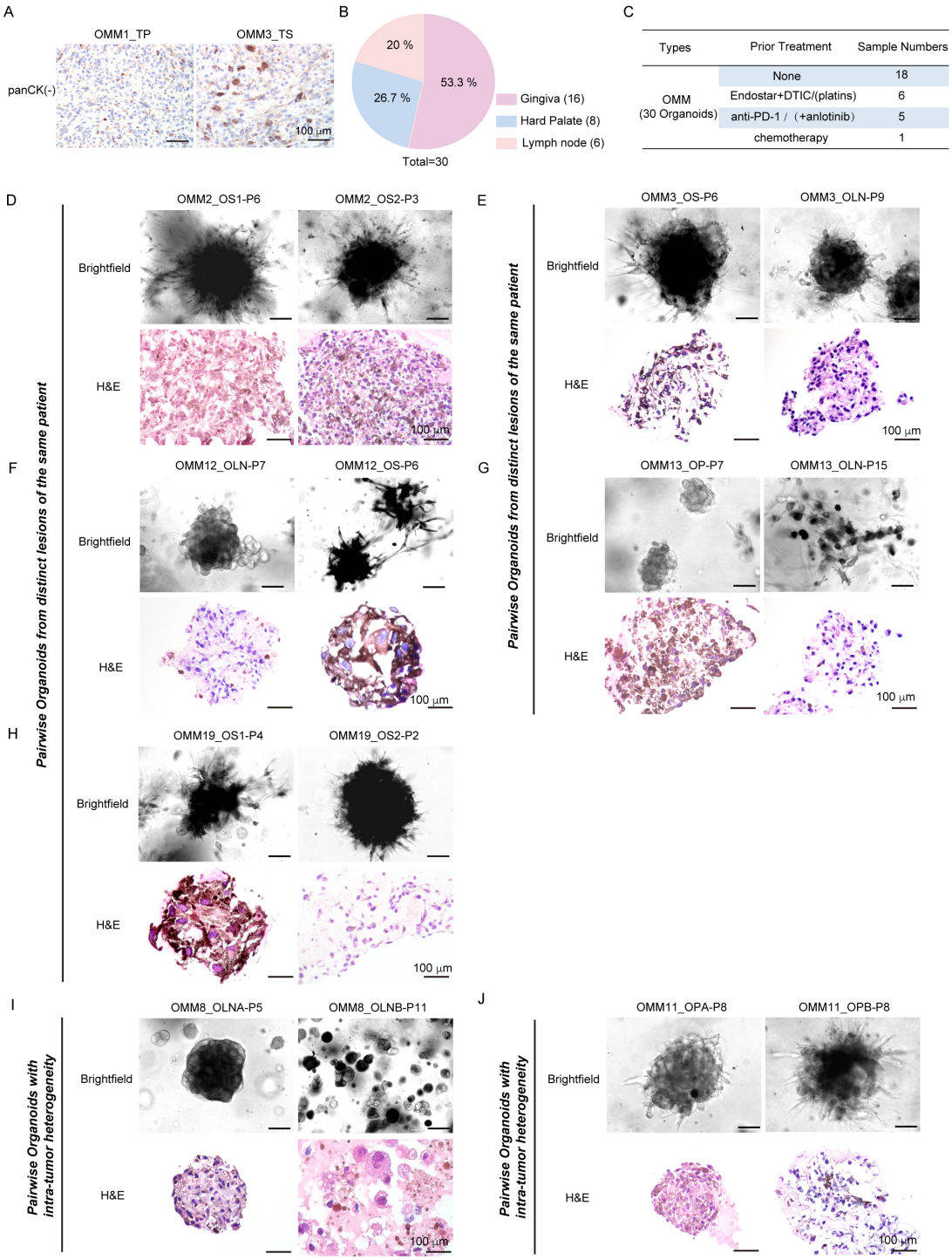

Fig. S1

Fig. S1. Summary of the generated organoids, bright-field images and H&E staining of groups of OMM organoids derived from chronologically and intratumorally distinct lesions of the same patient.

(A) PanCK staining in OMM1_TP and OMM3_TS. No positive signals for OMM tissues. Scale

bars, 100 μm. **(B-C)** Overview of the clinical information in parental tumors of OMM organoids. The anatomical location **(B)**; Prior drug treatment to the parental tissues before OMM organoids generation **(C)**. **(D-H)** Bright-field images and H&E staining of OMM organoids from one individual of different disease stages. Images of OMM2 **(D)**; images of OMM3 **(E)**; images of OMM12 **(F)**; images of OMM13 **(G)**; images of OMM19 **(H)**. **(I-J)** Bright-field images and H&E staining of OMM organoids from different tumor regions in one individual. Images of OMM8 **(I)**; images of OMM11 **(J)**. For **(D-J)**, "-Pn" denoted "-Passage n"; Scale bars, 100 μm.

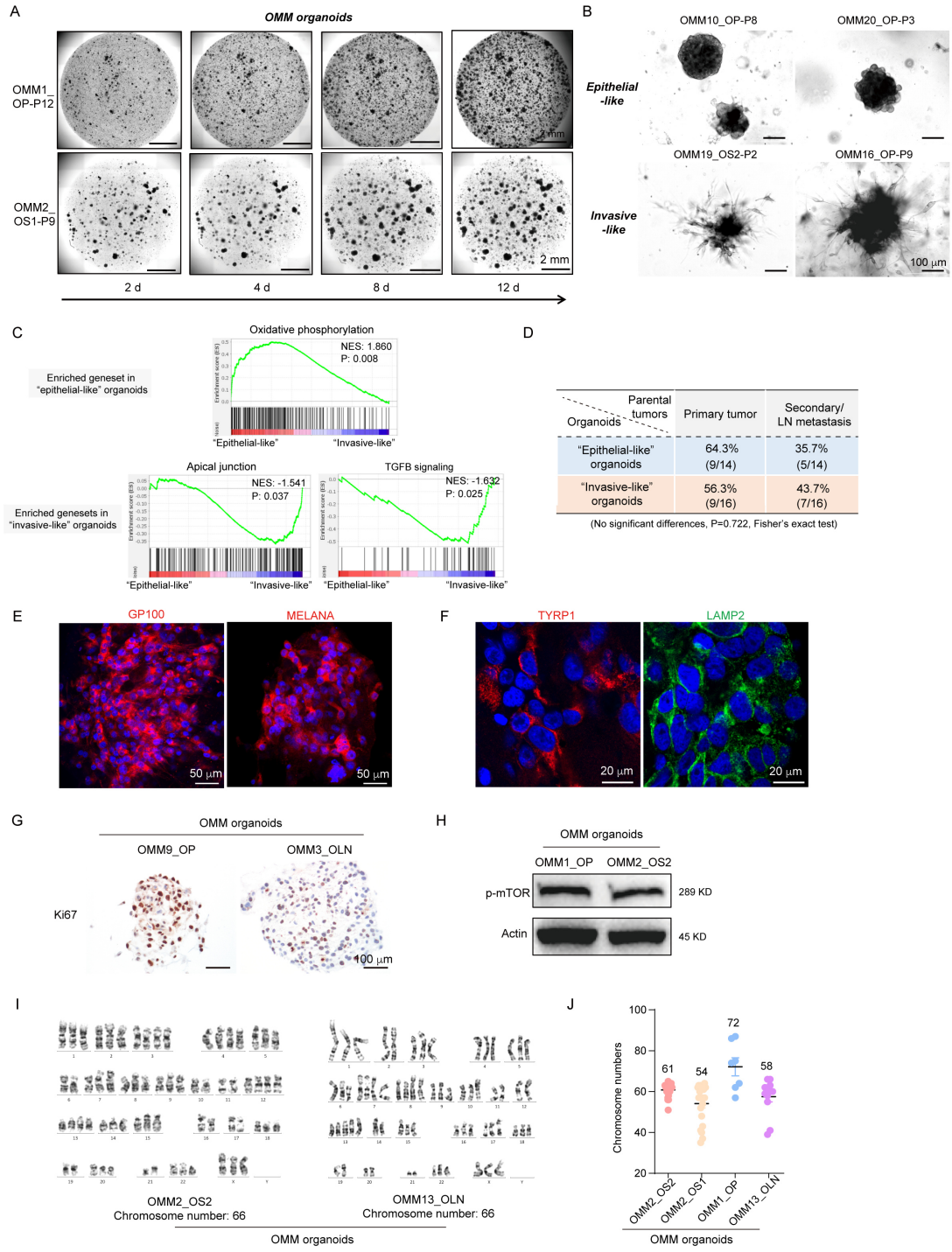

Fig. S2

Fig. S2. Additional proliferation and marker expression characteristics of OMM organoids.

(A) Representative images showing outgrowth of 2 organoids during culture. Images were taken starting from 1 day after initial plating and progressively taken on day 2, 4, 8 and 12. Scale bar: 2 mm. **(B)** Bright-field images of OMM organoids. 2 types of morphology were observed, one is epithelial-like; the other is invasive-like. Scale bars: 100 μm. **(C)** GSEA results showing the

genesets enrichment in “epithelial-like” and “invasive-like” OMM organoids. The NES and P-value are listed. NES: normalized enrichment score. $P < 0.05$ for the significance. (**D**) The clinical phenotypes of the parental tumor for “epithelial-like” and “invasive-like” organoids. No significant differences were observed between the two groups ($P = 0.722$, Fisher’s exact test). **(E)** IF staining of melanocytic marker GP100 and MELANA in OMM1_OP-P8 organoids. Scale bars, 50 µm. **(F)** IF staining of melanosome marker TYRP1 and LAMP2 in OMM10_OP-P8 organoids. Scale bars, 20 µm. **(G)** Ki67 staining in OMM9_OP-P12 and OMM3_OLN-P12. Scale bars, 100 µm. **(H)** Western blotting results showing phospho-mTOR expression in OMM organoids (P6). **(I)** Karyogram of representative G-banded metaphase stages for OMM2_OS2-P11 and OMM13_OLN-P26 organoids. **(J)** Chromosome numbers distribution and median chromosome numbers based on the metaphase spreads of OMM organoids (OMM2_OS2-P11; OMM2_OS1-P13; OMM1_OP-P22; OMM13_OLN-P26). For (**A-J)**, “-Pn” denoted “-Passage n” in figures.

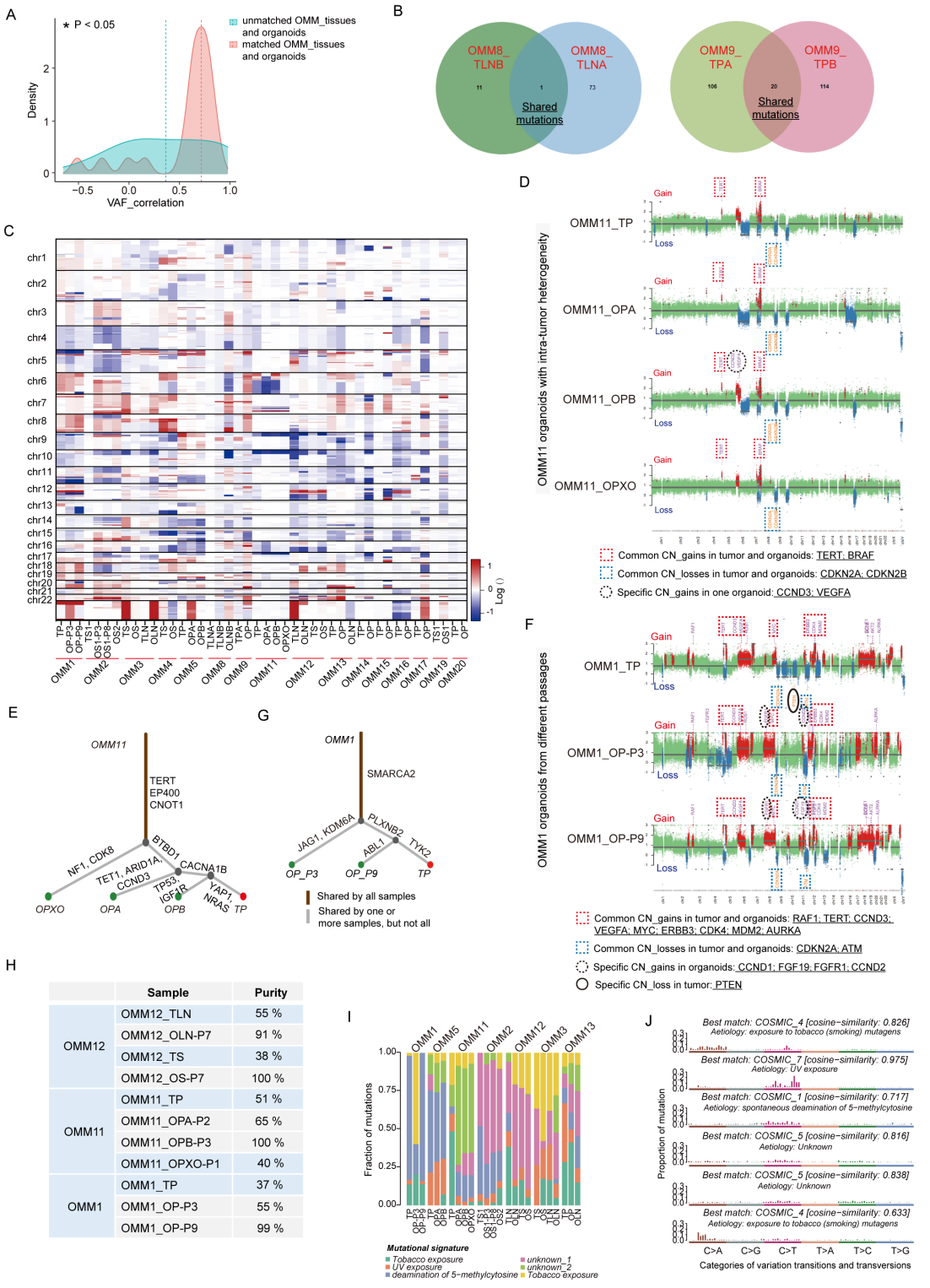

	Sample	Purity
OMM12	OMM12_TLN	55 %
	OMM12_OLN-P7	91 %
	OMM12_TS	38 %
	OMM12_OS-P7	100 %
OMM11	OMM11_TP	51 %
	OMM11_OPA-P2	65 %
	OMM11_OPB-P3	100 %
	OMM11_OPXO-P1	40 %
OMM1	OMM1_TP	37 %
	OMM1_OP-P3	55 %
	OMM1_OP-P9	99 %

Fig. S3

Fig. S3. Additional information of genetic alterations in OMM organoids and their parental tumors.

(A) Distributions of Pearson's correlation coefficients from matched and unmatched OMM organoids and OMM tissues. Vertical dashed lines represented the median coefficients. P-value =

0.049, Wilcoxon rank sum test. **(B)** Venn plots showing concordant somatic mutations in two samples of intra-tumor heterogeneity from one individual. **(C)** Heatmap showing genome wide DNA copy number alteration status of OMM organoids and their parental tumors. **(D-G)** Scatter plots illustrating genome wide CNAs and phylogenetic trees showing somatic mutations of OMM tissue-organoid pairs in OMM11 **(D-E)** and OMM1 **(F-G)**. **(H)** Tumor purity in OMM tissues and generated organoids via CNVs and mutations analysis with the ABSOLUTE software. **(I)** Mutational signature decomposition analysis in OMM groups with different disease stages, passage numbers or intra-tumor heterogeneity. Among the 30 signatures, the top 6 signatures representing the majority of mutations with cosine similarities > 0.6 were shown. **(J)** An exhibition of the top 6 signatures that represented the majority of mutations in OMM organoids and their parental tumors.

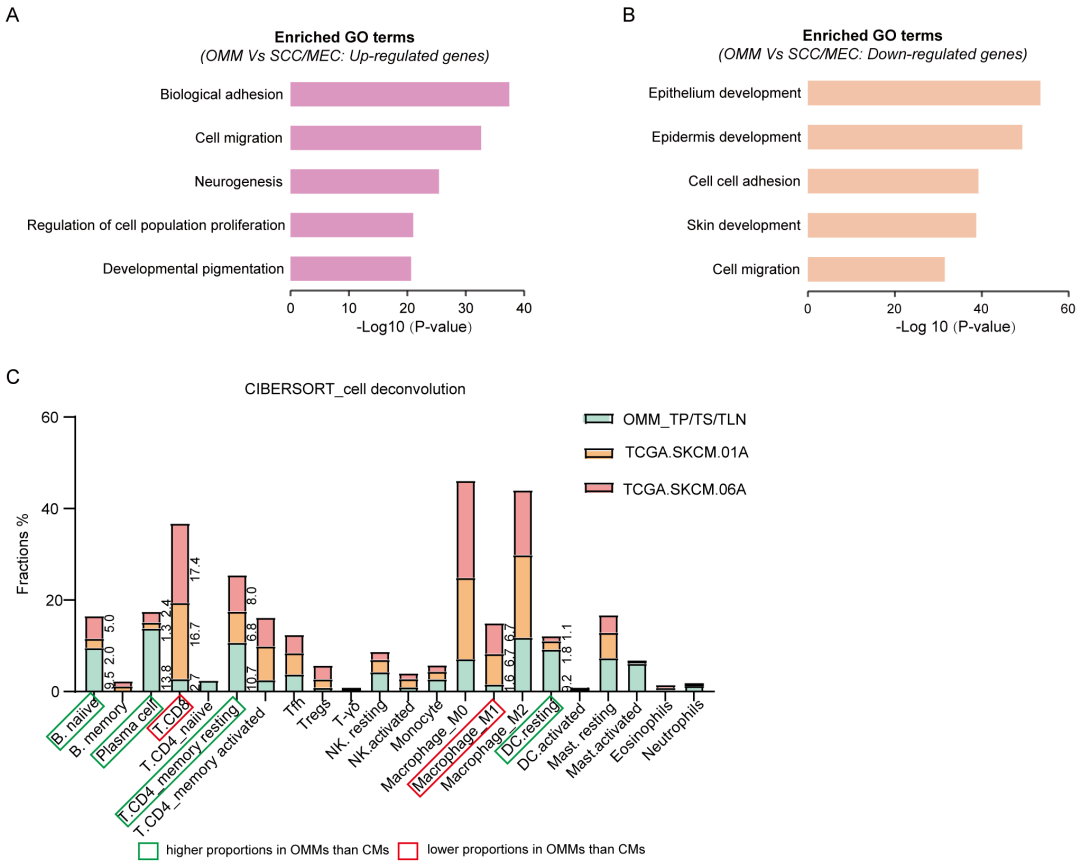

Fig. S4

Fig. S4. Additional transcriptome analysis of OMMs and the corresponding organoid lines. **(A-B)** GO terms for enriched pathways in OMM organoids **(A)** or SCC/MEC organoids **(B)** after comparison. P-value (< 0.05) was used to calculate enrichment. **(C)** Deconvolution of cell types in our OMM tissues (OMM_TP/TS/TLN) and the skin cutaneous melanoma (SKCM) tissues in the TCGA_cohort with the transcriptome data using CIBERSORT. Note that 01A represented primary CM; 06A represented recurrent CMs. The proportions of immune cells are provided on the right side of the columns.

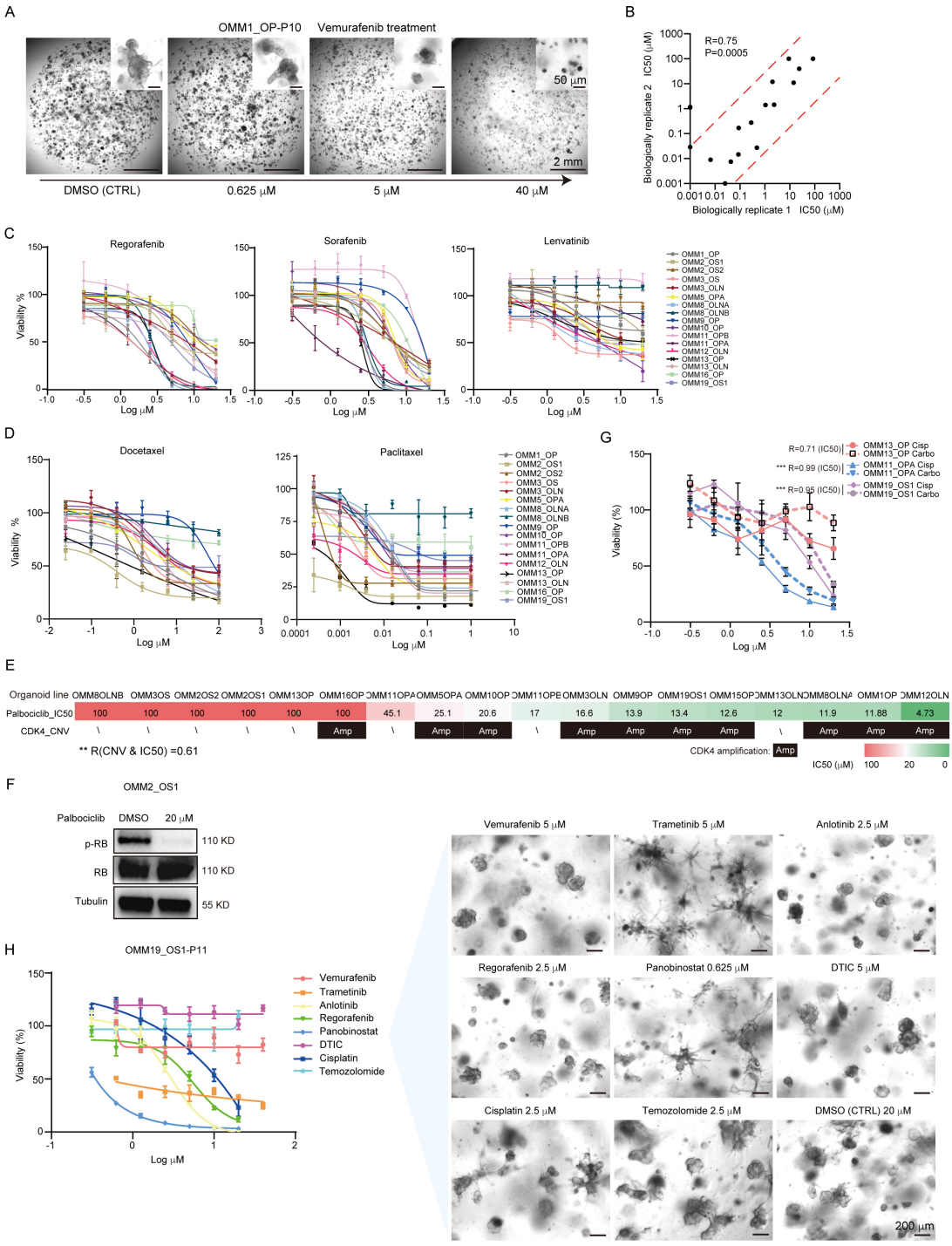

Fig. S5

Fig. S5. OMM organoids served as a platform for drug screening.

(A) Bright-field images of organoids' response to vemurafenib of different concentrations. Cell viability was increased upon gradually-decreased drug concentration. **(B)** Scatterplot showed the Pearson correlation of IC50 values for biological replicates of drug screening data. Cells at early or later passages were involved in the replicates. R = 0.75, P < 0.05. Each dot represents one OMM

organoid line. **(C-D)** Dose response curves for OMM organoids treated with regorafenib, sorafenib and lenvatinib **(C)**; docetaxel, paclitaxel **(D)**. **(E)** List of OMM organoids ranked on the basis of response to palbociclib (a CDK4 inhibitor) from higher IC50 to lower IC50. The *CDK4* CNV status were correspondingly exhibited. The Pearson correlation of CNV alteration and IC50 values were indicated. R = 0.61, **P < 0.01. **(F)** Western blotting results showing the inhibition of phospho-RB in OMM2_OS1-P9 organoid treated with 20 μM palbociclib. **(G)** Dose response curves for OMM organoids treated with cisplatin and carboplatin. ***P < 0.001. **(H)** Dose response curves for OMM19_OS1 organoids treated with several drugs (left). The morphological structures of organoids were shown after treatment of these drugs at the concentrations that nearest IC50 value (right). Scale bars, 200 μm. For (**C**-**D**) and (**G**-**H**), Data presented as the mean ± SD, n = 4 biologically independent replicates for each data point.

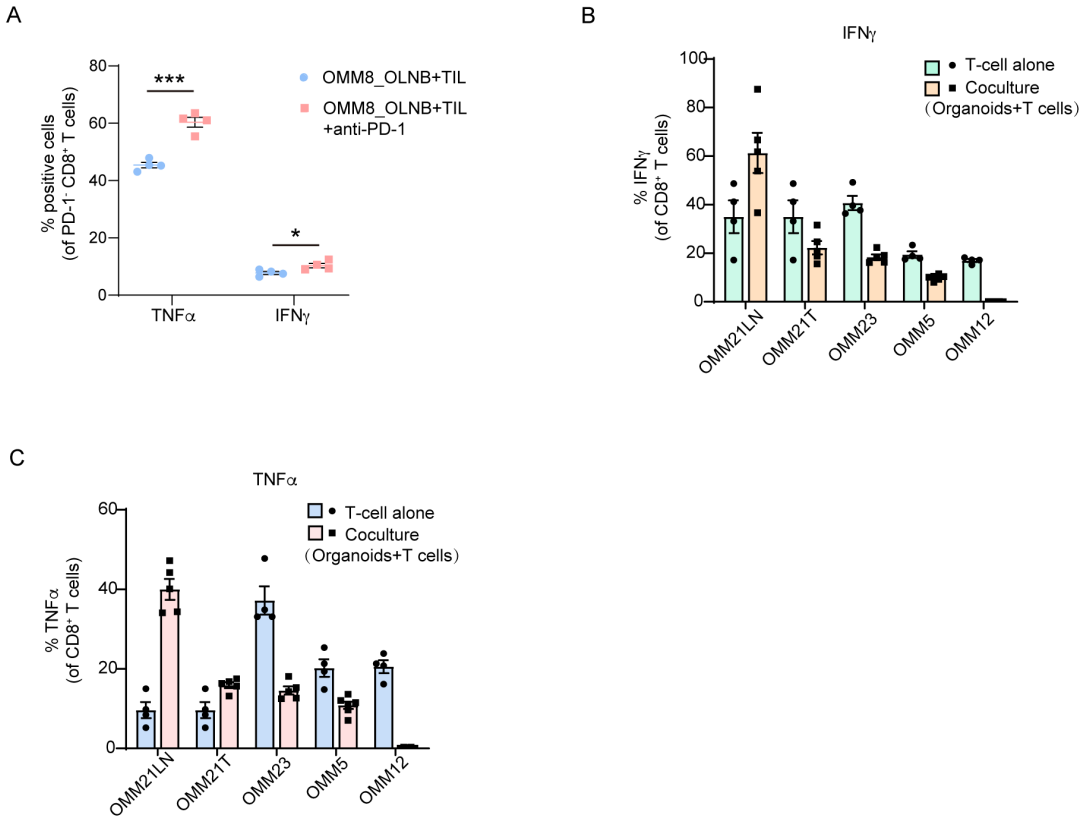

Fig. S6

Fig. S6. Summary of T cell activities when culture alone and coculture with OMM organoids. (**A**) The percentages of PD-1$^-$ & CD8$^+$ T cells positive for TNFα and IFNγ in the OMM8_OLNB-P11 organoid and T cell coculture group. Data is presented as the mean ± SEM (n = 4, biologically independent replicates). **(B-C)** The percentages of CD8$^+$ T cells positive for IFNγ (**B**) and TNFα (**C**) in the proliferated T-cell populations or in the OMM organoids and T cell coculture system. Data were presented as the mean ± SEM (n = 4~5, biologically independent replicates).

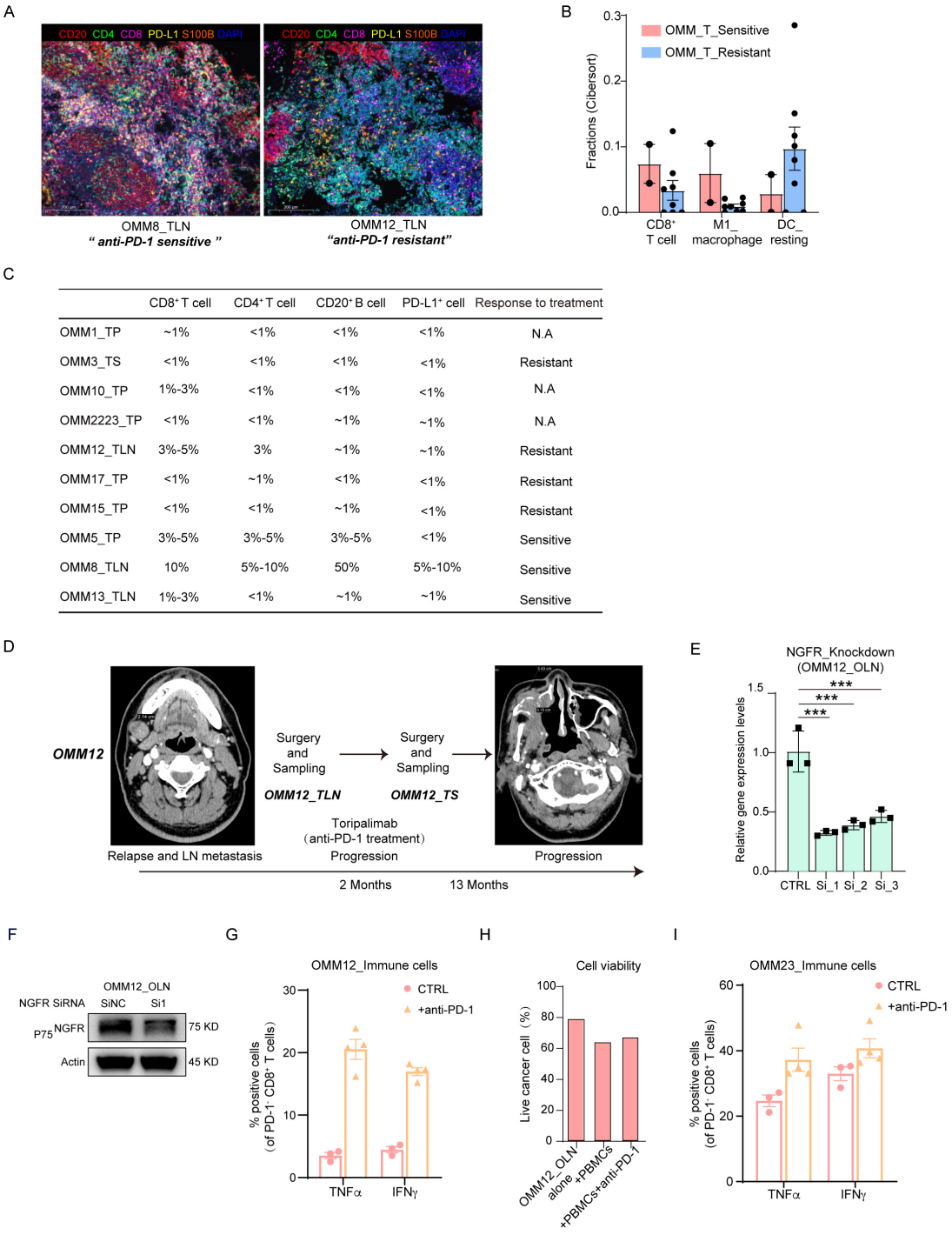

	CD8⁺ T cell	CD4⁺ T cell	CD20⁺ B cell	PD-L1⁺ cell	Response to treatment
OMM1_TP	~1%	<1%	<1%	<1%	N.A
OMM3_TS	<1%	<1%	<1%	<1%	Resistant
OMM10_TP	1%-3%	<1%	<1%	<1%	N.A
OMM2223_TP	<1%	<1%	~1%	~1%	N.A
OMM12_TLN	3%-5%	3%	~1%	~1%	Resistant
OMM17_TP	<1%	~1%	<1%	<1%	Resistant
OMM15_TP	<1%	<1%	~1%	<1%	Resistant
OMM5_TP	3%-5%	3%-5%	3%-5%	<1%	Sensitive
OMM8_TLN	10%	5%-10%	50%	5%-10%	Sensitive
OMM13_TLN	1%-3%	<1%	~1%	~1%	Sensitive

Fig. S7

Fig. S7. Difference of cell fractions, drug responses and T cell activities between anti-PD-1 resistant and anti-PD-1 sensitive groups.

(A) Multiple IHC results of OMM8_TLN and OMM12_TLN showing the expression levels of CD20, CD8, CD4, PD-L1, and S100B. Red for CD20, green for CD4, violet for CD8, yellow for PD-L1, and orange for S100B. Scale bars, 200 μm. **(B)** Deconvolution of cell types in our OMM

tissues which were sensitive or resistant to anti-PD-1 antibody with the transcriptome data using CIBERSORT. **(C)** Quantitation of immunohistochemistry staining results of $CD8^+$, $CD4^+$ T cells, $CD20^+$ B cells and PD-$L1^+$ cells in OMM tissues. **(D)** The radiation examination and therapeutic schedule for the parental tumors of OMM12 in the clinic. **(E)** Knockdown efficiencies of NGFR siRNAs in OMM12_OLN-P16 were determined by qPCR. Data is presented as the mean ± SD. A two-tailed unpaired Student's t-test was used for the P-values. ***P < 0.001. (**F**) Knockdown efficiencies of NGFR siRNAs in OMM12_OLN-P16 were determined by western blot (Protein levels of (NGFR/Actin) in SiNC:Si1 = 1:0.78). (**G**) The percentages of PD-1^- & $CD8^+$ T cells positive for IFNγ and TNFα in the PBMCs of OMM12 with or without addition of nivolumab. Data presented as the mean ± SEM (n = 3~4, biologically independent replicates). **(H)** Live cell proportions of tumor cells in the OMM12_OLN small clumps after co-culture with autologous PBMC cells with or without nivolumab addition. **(I)** The percentages of PD-1^- & $CD8^+$ T cells positive for IFNγ and TNFα in the PBMCs of OMM23 with or without addition of ant-PD-1 antibody. Data presented as the mean ± SEM (n = 3~4, biologically independent replicates).

Supplementary Table Legends

Table S1. Dissociation trials for OMM organoids

Table S2. Patient clinical data for the organoids of short-term passages (< P5)

Table S3. Patient clinical data for the successfully generated organoids

Table S4. Drugs information and IC50 values in OMM organoids

Table S5. Genesets related to melanoma cell phenotypes

Table S6. Reagents and Resource information

Table S7. SiRNAs and primers information